Chemical Science

ROYAL SOCIETY OF CHEMISTRY

EDGE ARTICLE

View Article Online
View Journal | View Issue

Cite this: *Chem. Sci.*, 2024, **15**, 16681

All publication charges for this article have been paid for by the Royal Society of Chemistry

Insight into the charge transfer behavior of an electrochemiluminescence sensor based on porphyrin–coumarin derivatives with a donor–acceptor configuration†

Hui Xiao, ‡[a] Yali Wang,‡[a] Yaqi Zhao,‡[a] Rongfang Zhang,[a] Kainan Kang,[a] Yanjun Feng,[a] Yuling Gao,[a] Huixia Guo,[a] Bingzhang Lu,*[b] Peiyao Du *[ab] and Xiaoquan Lu *[a]

The excellent photophysical and electrochemical properties of porphyrins have inspired widespread interest in the realm of electrochemiluminescence (ECL). The aggregation-caused deficiency of ECL emission in aqueous solution, however, still severely impedes further applications. Herein, a molecule with a donor–acceptor (D–A) configuration, ATPP–Cou, consisting of monoaminoporphyrin as an electron donor and coumarin as an electron acceptor, was designed as an ECL luminophore to address the susceptibility of the porphyrin to aggregation-caused quenching (ACQ) in aqueous solution. ATPP–Cou demonstrated a three-fold enhanced ECL signal compared to pristine ATPP. Despite the acknowledged significance of intramolecular charge transfer (ICT) in generating excited states in ECL, there is a lack of quantitative descriptions. Herein, intensity-modulated photocurrent spectroscopy (IMPS) and scanning photoelectrochemical microscopy (SPECM) were utilized to validate the influence of ICT on the enhancement performance of D–A type ECL molecules. Additionally, ATPP–Cou was also developed as a probe for the successful detection of Cu^{2+} in aqueous solution. The present study not only enriches the repertoire of efficient porphyrin-based ECL luminophores applicable in aqueous environments but also exemplifies the successful integration of novel measurement techniques to provide more comprehensive insights into the underlying mechanisms responsible for improved ECL performance.

Received 28th June 2024
Accepted 15th September 2024

DOI: 10.1039/d4sc04274c

rsc.li/chemical-science

1 Introduction

Electrochemiluminescence (ECL) is a process in which electrogenerated reactive species undergo electron-transfer reactions in the vicinity of the electrode surface to form excited states. Subsequently, these excited states return to their ground state and emit light.[1–5] Benefitting from its prominent advantages such as near-zero background, high sensitivity, simple instrumentation, fast response, excellent stability, and independence from external excitation sources,[6,7] ECL has garnered widespread interest, particularly in environmental analysis,[8,9] biosensing[10–15] and other fields.[16–18]

The utilization of highly efficient luminophores is currently a critical part in the development of ECL systems.[19] Organic molecules, due to their facile chemical modification, structural tailorability, and low metal content, have become prominent ECL emitters. Among them, the exceptional photophysical and electrochemical properties of porphyrins establish them as a classic organic ECL emitter.[20–22] The ECL of porphyrins in organic solutions has been reported by A. J. Bard and coworkers.[23] Our group exploited the cathodic ECL behaviors of *meso*-tetra(4-carboxyphenyl) porphyrin (TCPP) and *meso*-tetra(4-sulfonatophenyl)porphyrin (TSPP) in aqueous solution.[24,25] Nevertheless, conventional porphyrin luminophores often undergo severe aggregation-induced quenching (ACQ) due to strong aromatic π–π interactions, which results in the ECL efficiency in the aqueous phase often falling short of the desired level.[26] Structural modification is regarded as a promising way to overcome this limitation and fully leverage the inherent advantages of porphyrins. In our previous study, we successfully achieved the ACQ-to-AIE transformation of 5-(4-aminophenyl)-

[a]*Key Laboratory of Water Security and Water Environment Protection in Plateau Intersection (Ministry of Education), Key Laboratory of Bioelectrochemistry & Environmental Analysis of Gansu Province, College of Chemistry & Chemical Engineering, Northwest Normal University, Lanzhou 730070, P. R. China. E-mail: luxq@nwnu.edu.cn*

[b]*School of Chemical Engineering and Technology, Xi'an Jiaotong University, Shanxi 710049, P. R. China. E-mail: bingzhang@xjtu.edu.cn; peiyao@xjtu.edu.cn; peiyao.du@nwafu.edu.cn*

† Electronic supplementary information (ESI) available. See DOI: https://doi.org/10.1039/d4sc04274c

‡ These authors contributed equally to this work.

10,15,20-triphenyl-porphyrin (ATPP) by facile molecular decoration of an ATPP core with inherent AIE-active tetraphenylethene.[27] This modification resulted in an enhancement in ECL intensity compared to pure ATPP in aqueous solution. Despite recent progress, the development of novel, highly efficient, and readily accessible porphyrin-based ECL luminophores for implementation in aqueous environments, along with a comprehensive investigation into their emission mechanisms, remains an active and ongoing theme within the realm of ECL research. Coumarin and its derivatives are of great interest as electron acceptors in the fields of biology, solar cells, and organic light-emitting diodes primarily due to their high fluorescence quantum yield, low toxicity, and ease of modification.[28,29] We considered whether it is possible to combine porphyrin and coumarin to achieve efficient and stable ECL emitters in aqueous environments.

Typically, emitters such as small molecules and nanocrystals undergo transitions to excited states *via* charge transfer mechanisms.[30] Grasping how molecular arrangements can efficiently collect and transfer charges will enhance the design and refinement of electronic structures for emitters, leading to improved performance in ECL. Nonetheless, studies focusing on the charge transfer dynamics of ECL molecules, especially monomer emitters, are still sparse, largely because of the lack of effective electrochemical methods for *in situ* quantitative evaluation of charge transfer kinetics in these compounds.[31,32]

In this work, an aminoporphyrin–coumarin (ATPP–Cou) molecule with a donor–acceptor (D–A) system as an ECL emitter was synthesized through a Schiff-base reaction between a monoaminoporphyrin moiety as the electron donor and a coumarin moiety as the electron acceptor. Consequently, the ATPP–Cou molecule exhibits a significantly improved ECL signal compared to monoaminoporphyrin (ATPP). The transportation behavior of carriers in excited states was dynamically characterized using SPECM and IMPS, providing valuable insights for a more comprehensive understanding of ECL mechanisms. To the best of our knowledge, this is the first work that quantitatively studies the CT behavior in ECL through advanced *in situ* electrochemical methods. Furthermore, ATPP–Cou can be utilized for the sensitive and selective detection of Cu^{2+} in aqueous solution, with a detection limit of 0.64 nM.

2 Results and discussion

2.1 Preparation and characterization

5-(4-Aminophenyl)-10,15,20-triphenyl porphine (ATPP) and aldehyde–coumarin (Cou) were synthesized according to the previous literature[33,34] and used to construct a donor–acceptor type porphyrin derivative (ATPP–Cou) through a Schiff-base reaction, as described in Fig. 1a. The molecular structures were characterized using nuclear magnetic resonance spectroscopy and mass spectrometry (Fig. S1–S11†). The UV-vis absorption and photoluminescence (PL) properties of ATPP, coumarin, and ATPP–Cou were measured in diluted DMF. As shown in Fig. 1b, the absorption spectrum of ATPP showed a strong Soret band at 420 nm and four weak Q bands ranging from 500 to 700 nm, corresponding to the characteristic π–π* electron transition.

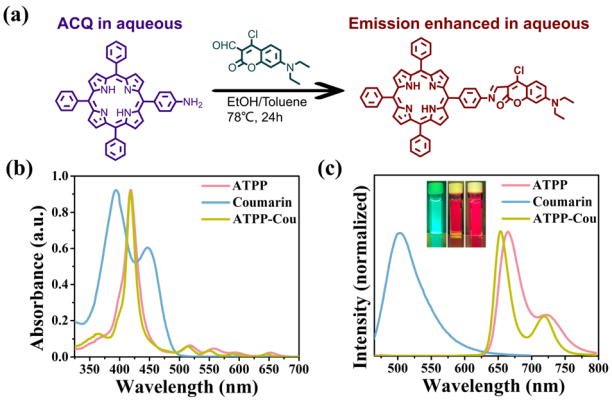

Fig. 1 (a) Synthesis of the donor–acceptor porphyrin derivative; (b) UV-vis absorption and (c) photoluminescence spectra of ATPP, coumarin, and ATPP–Cou in DMF (1×10^{-4} M); the inset shows their photography under a 365 nm ultraviolet lamp.

Notably, the absorption spectrum of ATPP–Cou notably exhibits features from both ATPP and coumarin. The narrowing of the Soret band and the blue shift of Q bands primarily arise from the incorporation of electron-withdrawing groups derived from coumarins. The PL spectra of ATPP, coumarin, and ATPP–Cou are presented in Fig. 1c, accompanied by the inserted photographs taken under a 365 nm ultraviolet lamp. The emission spectrum of ATPP–Cou exhibits two distinct peaks at 654 and 719 nm, respectively. In comparison to ATPP, a slight blue-shift (from 664 nm to 654 nm) is observed in the maximum peak, which can be attributed to the electron-withdrawing ability of the coumarin group.[35] The absence of the emission peak of Cou was observed in the ATPP–Cou molecule around 500 nm; meanwhile, the major absorption band of Cou in ATPP–Cou disappears and the Soret band becomes narrower compared to ATPP, suggesting effective electron coupling between Cou and ATPP.[36] The quantum yield (QY) measurements of ATPP and ATPP–Cou were also conducted in both solution and solid states. The QY of ATPP in the solid state was found to be only 0.34%, whereas it reached 5.73% in solution (DMF, 1×10^{-4} M), indicating significant aggregation-caused quenching (ACQ). As anticipated, the QY of ATPP–Cou exhibited an approximately twenty-fold increase (6.20%) compared to that of ATPP in the solid state. Furthermore, ATPP–Cou effectively mitigated ACQ and demonstrated an enhanced quantum yield of 9.23% in solution.

2.2 Electrochemiluminescence characterization

The CV and ECL-potential curves of different emitters and a bare GCE are shown in Fig. 2a and b (potential window of −1.7 V to −0.1 V, scan rate of 0.15 V s^{-1}, 0.1 M PBS with 0.1 M KCl as the supporting electrolyte, and $K_2S_2O_8$ as the co-reactant). As seen in Fig. 2a, the reduction peak of ATPP–Cou/$K_2S_2O_8$ occurred at about −0.79 V. It can be reduced to form the corresponding ATPP–Cou radical anions (ATPP–$Cou^{\bullet-}$). Finally, the strong oxidant $SO_4^{\bullet-}$ reacts with ATPP–$Cou^{\bullet-}$ to produce exited-state ATPP–Cou*, resulting in a strong ECL emission

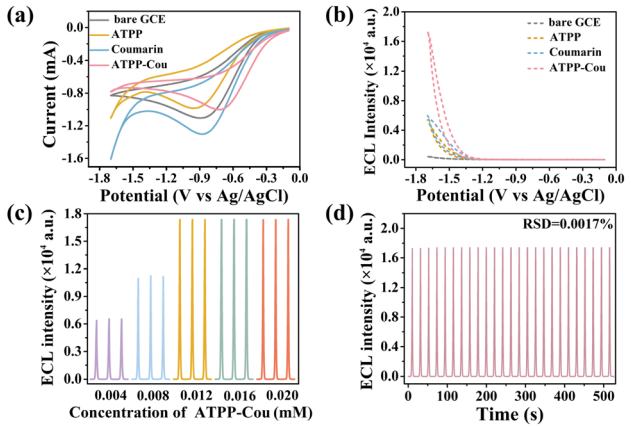

Fig. 2 (a) CV profiles with 0.1 M $K_2S_2O_8$; (b) ECL-potential curves; (c) ECL intensity of ATPP–Cou under different concentration conditions; (d) ECL intensity *vs.* time curve for the ATPP–Cou/$K_2S_2O_8$ system under optimal conditions for continuous 25 cycles.

when the exited state returns to the ground state. As we all know, $K_2S_2O_8$ is a commonly used cathode co-reactant in ECL reactions to trigger increased ECL. Under sufficiently negative potential conditions, $S_2O_8^{2-}$ undergoes decomposition to yield SO_4^{2-} and $SO_4^{\bullet-}$.[37] $K_2S_2O_8$ was utilized as a co-reactant in this work. Fig. S12† shows the CV curves of the bare GCE in 0.1 M PBS solution with/without $K_2S_2O_8$. There was no noticeable reduction peak for the bare GCE in PBS. During cathodic scanning, a distinct reduction peak at around −0.80 V appeared for the bare GCE in the presence of $K_2S_2O_8$, owing to the electrochemical reduction of $S_2O_8^{2-}$ to produce $SO_4^{\bullet-}$ and SO_4^{2-}. The ECL intensity of ATPP, Cou, and ATPP–Cou is compared in Fig. 2b. Obviously, the ATPP–Cou modified GCE exhibited relatively stronger cathodic ECL emission with an onset potential of approximately −1.3 V (pink dashed line) and maximum emission around −1.70 V in the presence of $K_2S_2O_8$.

In order to achieve the optimal ECL signal of ATPP–Cou in aqueous systems, several experimental settings are determined in detail. The potential window was first optimized because it is significant for triggering efficient ECL of the ATPP–Cou/$K_2S_2O_8$ system. The highest ECL intensity was observed within the potential range of −1.7 V to −0.1 V (Fig. S13a†). The influence of the scan rate on the ECL of the ATPP–Cou/$K_2S_2O_8$ system was also studied (Fig. S13b†). Initially, the ECL intensity exhibited an upward trend with increasing scan rates and reached a plateau above 150 mV s^{-1}. Lower scan rates were insufficient to capture the short lifetime of electrogenic radicals;[27] therefore, 150 mV s^{-1} was determined as the optimal scan rate. The ECL intensity of the ATPP–Cou/$K_2S_2O_8$ system increased proportionally with increasing $K_2S_2O_8$ concentration until it reached 0.1 M, at which point it remained constant (Fig. S13c†). This can be explained by the limited number of available light sources in the system, resulting in excess co-reactants being unable to fully participate in the ECL reaction. The ECL of the ATPP–Cou/$K_2S_2O_8$ system is also influenced by the pH of the supporting electrolyte, with the highest ECL signal observed at a pH of 6 (Fig. S13d†). At excessively high pH levels, the strong oxidant $SO_4^{\bullet-}$ undergoes consumption due to the scavenging effect of OH^- ions. The ECL intensity of the ATPP–Cou/$K_2S_2O_8$ system was ultimately optimized through adjustment of the concentration of the ATPP–Cou emitter (Fig. 2c). The intensity initially exhibited an increase within the concentration range of 0.004 mM to 0.012 mM, followed by a subsequent stabilization. Consequently, a concentration of 0.012 mM was chosen for all subsequent ECL experiments. As seen in Fig. S14†, the ECL signal of ATPP–Cou (17 370 a.u.) was much higher than that of ATPP and coumarin, thereby indicating that ATPP–Cou holds great potential for ECL detection in the aqueous phase. The stability of the ATPP–Cou/$K_2S_2O_8$ system was evaluated under 25 successive cyclic scans. Remarkably, the ECL signals exhibited negligible fluctuation with a relative standard deviation (RSD) of 0.0017% (Fig. 2d).

The ECL spectrum of ATPP–Cou was similar to that of ATPP, displaying two distinct emission peaks at 659 nm and 720 nm, as illustrated in Fig. 3a. Meanwhile, the ECL emission peak of coumarin was detected at 520 nm (Fig. 3b), suggesting that the ECL emission center of the ATPP–Cou molecule primarily originates from the porphyrin. To investigate the impact of the molecular electronic structure on ECL emission, DFT calculations were performed on ATPP and ATPP–Cou using the B3LYP functional and the 6-31+G(d) basis set. In the optimized configuration, the Cou moiety and ATPP are situated in the same plane and fully conjugated, indicating a strong electronic coupling of ATPP–Cou, which is consistent with the obtained photophysical results. The enhanced electronic coupling facilitates the electron transfer, thereby augmenting the probability of electrogenerated ECL.[38,39] The electron density in the HOMO of ATPP–Cou is primarily localized on the core of ATPP, whereas that in the LUMO is distributed throughout both ATPP and coumarin. The distribution of LUMO orbitals on coumarin, along with its conjugated system and strong electron-withdrawing groups, implies the potential formation of intramolecular charge transfer states between the coumarin moiety

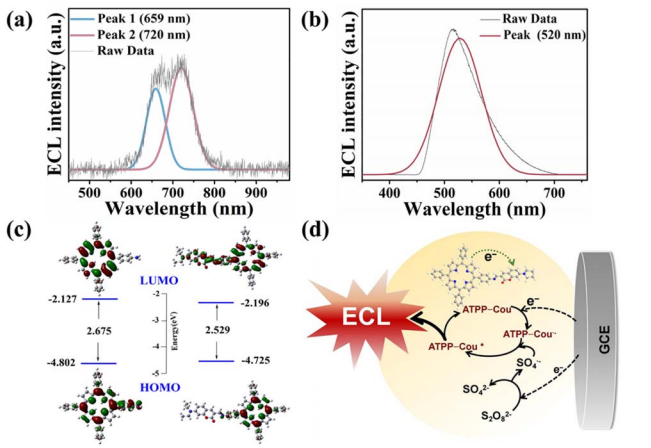

Fig. 3 ECL spectra of (a) ATPP–Cou and (b) coumarin (−2.7–2.2 V, in DCE solution with 0.1 M $TBAPF_6$); (c) molecular orbital isosurface plots and energy levels of the HOMO and LUMO for ATPP (left) and ATPP–Cou (right); (d) ECL mechanism of the ATPP–Cou/$K_2S_2O_8$ system.

and ATPP in this study. It is expected to facilitate the generation of excited states through enhanced charge transfer reactions in ECL. As depicted in Fig. 3c, the calculated HOMO–LUMO gap for the synthesized ATPP–Cou molecule (2.529 eV) is observed to be lower than that of ATPP (2.675 eV). The reduced energy gap of ATPP–Cou also promotes electron transfer, leading to the stabilization of intermediate states and efficient formation of radical anions.[40]

In addition, the introduction of the coumarin segment disrupted the molecular symmetry of the porphyrin, resulting in an accumulation of charges in the region where the symmetry was broken.[41] This redistribution of excess charges improves the efficiency of excited state formation, leading to an enhancement in the ECL signal.[42,43] From Fig. 3d, with the synergistic effect of pre-optimized potential excitation and a donor–acceptor configuration with fast electron transfer characteristics, $K_2S_2O_8$ is reduced to generate more strong oxidizing species $SO_4^{\bullet -}$ (eqn (1)). ATPP–Cou could obtain an electron to form ATPP–Cou$^{\bullet -}$ when the potential was scanned in the negative potential region (eqn (2)). Subsequently, further production of unstable excited states of ATPP–Cou* occurs through oxidation of ATPP–Cou$^{\bullet -}$ by $SO_4^{\bullet -}$ generated near the electrode (eqn (3)). Finally, the decay of ATPP–Cou* back to the ground state causes the generation of an ECL signal (eqn (4)). The possible ECL emission mechanism of ATPP–Cou is as follows:

$$S_2O_8^{2-} + e^- \rightarrow SO_4^{2-} + SO_4^{\bullet -} \quad (1)$$

$$\text{ATPP–Cou} + e^- \rightarrow \text{ATPP–Cou}^{\bullet -} \quad (2)$$

$$\text{ATPP–Cou}^{\bullet -} + SO_4^{\bullet -} \rightarrow \text{ATPP–Cou}^* + SO_4^{2-} \quad (3)$$

$$\text{ATPP–Cou}^* \rightarrow \text{ATPP–Cou} + h\nu \quad (4)$$

The process of CT is fundamental to ECL, as it exerts a substantial influence on the efficiency of electron transfer between the electrically generated active intermediates, which is essential for the formation of the excited state. To thoroughly investigate the carrier's behavior of D–A type porphyrin molecules, specific and dynamic characteristic methods are still required in response to the aforementioned mechanism. A powerful *in situ* electrochemical technique, self-constructed UV-vis/SPECM, has been utilized to directly quantify the kinetic information of electron transfer.[44] In the SPECM measurement process, spin-coated ATPP and ATPP–Cou on the FTO substrates were used as the research object, with $K_3[Fe(CN)_6]_3$ chosen as the probe molecule using feedback mode (Fig. 4a). The probe approach curves under both light and dark conditions are depicted in Fig. 4b. Under photoexcitation, a "positive feedback" approach curve emerged as the probe current increased due to the regeneration of Fe(III) at the tip, suggesting a rapid transfer of photoelectrons between Fe(III) and the surface of porphyrin-derivative films on the FTO substrate. In contrast, a "negative feedback" curve was observed under the dark conditions. Compared to ATPP, ATPP–Cou exhibited a lower positive feedback current. And their respective kinetic rate constants (K_{eff}) were determined through data fitting (Table S1†).[45] The K_{eff} of ATPP (9.78×10^{-2} cm s^{-1}) exhibited a higher value compared to that of ATPP–Cou (8.38×10^{-2} cm s^{-1}), indicating that more photogenerated charge "escaped" from ATPP towards the surface and indirectly evidencing an elevated bulk charge transfer and excited state formation rate for ATPP–Cou. IMPS is another technique that effectively evaluates surface charge separation and recombination. The electron transport time (τ_d) can be estimated using the formula: $\tau_d = 1/(2\pi f_{min})$,[46] where f_{min} represents the frequency of the minimum point in the IMPS semicircle. As shown in Fig. 4c and d, the τ_d values for ATPP and ATPP–Cou were calculated to be 0.76 ms and 2.30 ms, respectively (Table S2†). Notably, the τ_d value of ATPP–Cou is three times higher than that of ATPP, suggesting a reduced electron transport rate to the surface during photoexcitation.[47] The observed difference indicates that, as a result of the introduction of coumarin, charges may exhibit a preference for intramolecular transfer rather than surface/interface transfer in the excited state. As we know, in ECL, efficient intramolecular charge transfer can enhance the efficiency of the excited state formation during electrochemical reactions. Therefore, the design of ECL organic luminophores with a donor–acceptor structure has the potential to change charge transfer characteristics, reduce the non-radiative decay, and enhance the efficiency and stability of excited state generation, ultimately resulting in an overall improvement in luminous efficiency and ECL intensity.

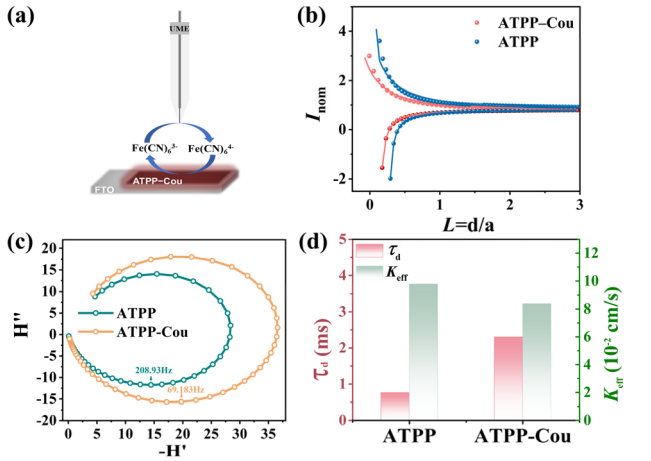

Fig. 4 (a) Schematic illustration of the testing process using SPECM. (b) Probe approach curves of ATPP and ATPP–Cou. (c) IMPS response curves recorded in PBS solution. (d) τ_d and K_{eff} values of ATPP and ATPP–Cou.

The fluorescence lifetime is closely related to the migration process of photoinduced carriers.[48] The time-resolved decay spectra of coumarin, ATPP, and ATPP–Cou were recorded (Fig. 5a and Table S3†), yielding lifetimes of 1.60 ns, 3.06 ns, and 9.13 ns, respectively. The prolonged lifetime indicates an extended π-conjugation and a highly efficient charge transfer of the D–A molecule, facilitating the generation of a greater amount of ATPP–Cou$^{\bullet -}$ in proximity to the electrode and resulting in enhanced ECL. The emission spectra of ATPP–Cou were studied in solvents with varying polarities to confirm the

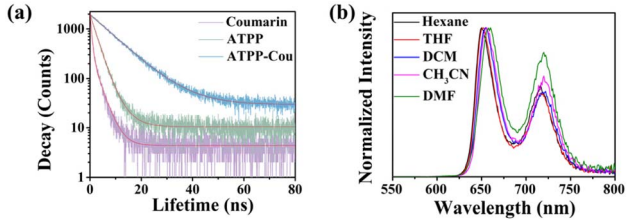

Fig. 5 (a) Fluorescence lifetime spectra of coumarin, ATPP and ATPP–Cou; (b) emission spectra of ATPP–Cou in solvents with varying polarities.

presence of intramolecular charge transfer. The emission peak of ATPP–Cou displayed a noticeable red-shift as the solvent polarity increased, with wavelengths of 649 nm (hexane), 651 nm (THF), 654 nm (DCM), 655 nm (CH_3CN), and 660 nm (DMF). Both theoretical and experimental findings provide further evidence that ATPP–Cou with a D–A type configuration undergoes intramolecular charge transfer upon excitation. The ECL efficiency of the ATPP–Cou/$K_2S_2O_8$ system was determined by calculating the number of injected electrons and emitted photons using the $Ru(bpy)_3^{2+}$ standard method.[49] The ECL efficiency of ATPP–Cou is calculated to be 80.6%, showing the significantly improved ECL performance of the D–A configuration proposed in this work. The calculation formula for ECL efficiency is as follows:

$$\varphi_{ECL} = \frac{\left(\frac{\int \text{ECL intensity d}t}{\int \text{Current d}t}\right)_x}{\left(\frac{\int \text{ECL intensity d}t}{\int \text{Current d}t}\right)_{st}}$$

2.3 Electrochemiluminescence detection of Cu^{2+}

Cu^{2+} is widely recognized as a common environmental contaminant among heavy metals.[50] Meanwhile, both an excess and a deficiency of Cu^{2+} in humans can result in liver/kidney damage, Alzheimer's disease, Wilson's disease, *etc.* Therefore, detecting Cu^{2+} is of utmost importance for biological health and environmental monitoring. Considering the advantages of the ECL method and the exceptional ECL performance exhibited by the ATPP–Cou/$K_2S_2O_8$ system, we employed ATPP–Cou/$K_2S_2O_8$ to fabricate an ECL sensor for ultrasensitive detection of Cu^{2+}. As shown in Fig. 6a, a favorable linear relationship between the ECL intensity and the natural logarithm value of Cu^{2+} concentration in the range of 10–385 nM is realized. The detection limit of our proposed ECL sensor was calculated to be 0.64 nM (S/N = 3), which was superior to that of other Cu^{2+} sensors reported in the literature (Table S4†). To evaluate the selectivity of the ECL sensor, a series of common cations (K^+, Zn^{2+}, Co^{2+}, Al^{3+}, Cd^{2+}, Cr^{6+}, Fe^{2+}, Mg^{2+}, Mn^{2+}, and Na^+) were chosen at a concentration 10 times higher than that of Cu^{2+} (Fig. 6c). The ECL intensity of the ATPP–Cou/$K_2S_2O_8$ system is significantly quenched only by Cu^{2+}, demonstrating the exceptional selectivity of the constructed ECL sensor. Sensors based on porphyrin derivatives are commonly used for detecting copper

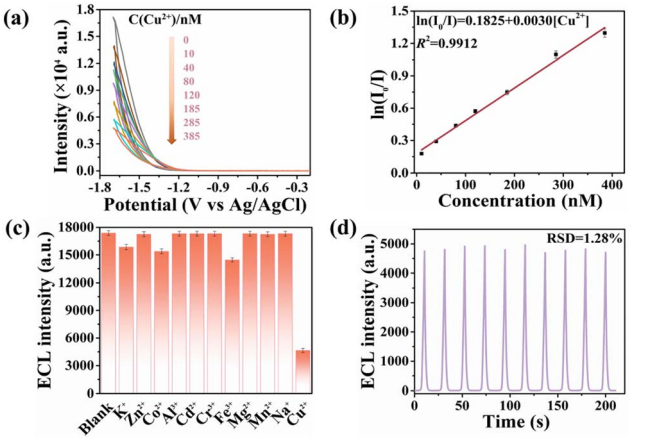

Fig. 6 (a) The ECL intensity–potential profiles of the proposed sensor in the presence of different Cu^{2+} concentrations; (b) the corresponding calibration curve; (c) comparison of the quenching effect of various metal ions on the ATPP–Cou/$K_2S_2O_8$ system; (d) stability of the designed ECL sensor in the presence of Cu^{2+}.

ions due to the complexation between copper ions and the nitrogen atoms of pyrrole in the porphyrin ring.[25] Another possible reason for this high selectivity is the paramagnetic nature of Cu^{2+}, which facilitates reversible electron transfer in the system and consequently leads to fluorescence quenching.[51] Alternatively, Cu^{2+} can potentially induce electron spin–orbit coupling and convert the excited singlet state into a triplet state, resulting in fluorescence quenching through internal conversion. The stability of the proposed ECL sensor was assessed by continuously scanning for 10 cycles in the presence of a 385 nM Cu^{2+} solution (0.1 M PBS, pH = 6.0). As depicted in Fig. 6d, the ECL intensity exhibited negligible fluctuations with a relative standard deviation (RSD) of only 1.28%. To evaluate the potential applicability of this ECL system in detecting Cu^{2+}, we collected samples of river water and performed recovery tests by introducing varying concentrations of Cu^{2+} (15, 55, and 75 nM). Acceptable recoveries from 96.9% to 100.2% were acquired (Table S5†).

3 Conclusions

In conclusion, an organic molecule with a D–A configuration was designed as an ECL emitter by integrating a porphyrin and coumarin as donor and acceptor units, respectively. Compared to the pristine porphyrin, the ECL signal of the coumarin-modified porphyrin is enhanced threefold in aqueous environments. More importantly, the ECL-enhanced mechanism was investigated in terms of charge transfer using IMPS and SPECM. The results indicate that ATPP–Cou enhances the ECL signal primarily due to improved intramolecular charge transfer, which is consistent with DFT calculation. Benefiting from the strong ECL emission of the ATPP–Cou/$K_2S_2O_8$ system and the quenching effect of Cu^{2+} on the ECL signal, a convenient sensor for Cu^{2+} was developed with a detection limit of 0.64 nM. Overall, our work not only offers an approach to studying the influence of the donor–acceptor molecules on ECL properties

but also enriches highly efficient porphyrin-based ECL luminophores.

Data availability

The data supporting this article have been included in the ESI.† Additional data are available upon request from the corresponding author.

Author contributions

H. Xiao and Y. Wang: conceptualization, investigation and data curation. Y. Zhao, R. Zhang and K. Kang: formal analysis and data curation. H. Guo, Y. Feng and Y. Gao: methodology. P. Du and H. Xiao: writing – original draft. B. Lu. and P. Du: writing – review & editing. X. Lu: validation, supervision and resources. All authors discussed the results and assisted during manuscript preparation.

Conflicts of interest

There are no conflicts to declare.

Acknowledgements

This work was supported by the National Natural Science Foundation of China (22174110, 22127803, 22222408, and 52370198), the Industrial Support Plan of the Gansu Provincial Department of Education (2021cyzc-01), and the Special Fund Project for Guiding Local Scientific and Technological Development by the Central Government (No. 2020-2060503-17). This research was also supported by the Engineering Laboratory of Electrochemical Technology & Nanodevice of Gansu Province and the Scientific Research Ability Improvement Program of Northwest Normal University (NWNU-LKQN2023-07).

Notes and references

1 J. R. Adsetts, K. Chu, M. Hesari, J. Ma and Z. Ding, *Anal. Chem.*, 2021, **93**, 11626–11633.
2 K. M. Omer, S. Y. Ku, K. T. Wong and A. J. Bard, *J. Am. Chem. Soc.*, 2009, **131**, 10733–10741.
3 Y. Liu, W. Guo and B. Su, *Chin. Chem. Lett.*, 2019, **30**, 1593–1599.
4 J. Descamps, Y. Zhao, B. Goudeau, D. Manojlovic, G. Loget and N. Sojic, *Chem. Sci.*, 2024, **15**, 2055–2061.
5 J. Cheng, L. Yang, R. Wang, J. A. Wisner, Z. Ding and H.-B. Wang, *Chem. Sci.*, 2024, **15**, 12291–12300.
6 J. Guo, M. Xie, P. Du, Y. Liu and X. Lu, *Anal. Chem.*, 2021, **93**, 10619–10626.
7 X. Xiong, C. Xiong, Y. Gao, Y. Xiao, M. M. Chen, W. Wen, X. Zhang and S. Wang, *Anal. Chem.*, 2022, **94**, 7861–7867.
8 W. R. Cui, Y. J. Li, Q. Q. Jiang, Q. Wu, Q. X. Luo, L. Zhang, R. P. Liang and J. D. Qiu, *Anal. Chem.*, 2021, **93**, 16149–16157.
9 X. L. Mao, Q. X. Luo, Y. J. Cai, X. Liu, Q. Q. Jiang, C. R. Zhang, R. P. Liang and J. D. Qiu, *Anal. Chem.*, 2023, **95**, 10803–10811.
10 W. Huang, G. B. Hu, W. B. Liang, J. M. Wang, M. L. Lu, R. Yuan and D. R. Xiao, *Anal. Chem.*, 2021, **93**, 6239–6245.
11 Y. Liu, H. Zhang, B. Li, J. Liu, D. Jiang, B. Liu and N. Sojic, *J. Am. Chem. Soc.*, 2021, **143**, 17910–17914.
12 Y. Fang, Z. Zhou, Y. Hou, C. Wang, X. Cao, S. Liu, Y. Shen and Y. Zhang, *Anal. Chem.*, 2023, **95**, 6620–6628.
13 Y. Liu, Y. Yao, B. Yang, Y. J. Liu and B. Liu, *Chin. Chem. Lett.*, 2022, **33**, 2705–2707.
14 F. Yin, E. Yang, X. Ge, Q. Sun, F. Mo, G. Wu and Y. Shen, *Chin. Chem. Lett.*, 2024, **35**, 108753.
15 L. Wang, J. Song, X. Wang, H. Qi, Q. Gao and C. Zhang, *Chin. Chem. Lett.*, 2020, **31**, 2520–2524.
16 M. H. Jiang, S. K. Li, X. Zhong, W. B. Liang, Y. Q. Chai, Y. Zhuo and R. Yuan, *Anal. Chem.*, 2019, **91**, 3710–3716.
17 Z. Han, M. Chai, X. Yu, J. Wang, Y. Zhao, A. Zhao and X. Lu, *Anal. Chem.*, 2023, **95**, 7036–7044.
18 Z. Zhang, P. Du, G. Pu, L. Wei, Y. Wu, J. Guo and X. Lu, *Mater. Chem. Front.*, 2019, **3**, 2246–2257.
19 J. Li, M. Xi, L. Hu, H. Sun, C. Zhu and W. Gu, *Anal. Chem.*, 2024, **96**, 2100–2106.
20 Y. Zhao, A. Zhao, Z. Wang, Y. Xu, Y. Feng, Y. Lan, Z. Han and X. Lu, *Anal. Chem.*, 2023, **95**, 11687–11694.
21 Y. Xu, Z. Han, P. Du and X. Lu, *TrAC, Trends Anal. Chem.*, 2023, **165**, 117136.
22 Z. Han, L. Zhang and X. Lu, *J. Chem. Educ.*, 2024, **101**, 1248–1256.
23 N. E. Tokel, C. P. Keszthelyi and A. J. Bard, *J. Am. Chem. Soc.*, 1972, **94**, 4872–4877.
24 D. Luo, B. Huang, L. Wang, A. M. Idris, S. Wang and X. Lu, *Electrochim. Acta*, 2015, **151**, 42–49.
25 J. Zhang, S. Devaramani, D. Shan and X. Lu, *Anal. Bioanal. Chem.*, 2016, **408**, 7155–7163.
26 Q. Han, C. Wang, Z. Z. Li, J. L. Wu, P. K. Liu, F. J. Mo and Y. Z. Fu, *Anal. Chem.*, 2020, **92**, 3324–3331.
27 Y. Zhang, Y. Zhao, Z. Han, R. Zhang, P. Du, Y. Wu and X. Lu, *Angew. Chem., Int. Ed.*, 2020, **59**, 23261–23267.
28 H. Liu, L. Wang, H. Gao, H. Qi, Q. Gao and C. Zhang, *ACS Appl. Mater. Interfaces*, 2017, **9**, 44324–44331.
29 Q. Han, N. Wang, M. Wang and J. Wang, *Sens. Actuators, B*, 2023, **393**, 134296.
30 W. Zhao, H.-Y. Chen and J.-J. Xu, *Chem. Sci.*, 2021, **12**, 5720–5736.
31 R. Luo, H. Lv, Q. Liao, N. Wang, J. Yang, Y. Li, K. Xi, X. Wu, H. Ju and J. Lei, *Nat. Commun.*, 2021, **12**, 6808.
32 X. Gao, G. Jiang, C. Gao, A. Prudnikau, R. Hübner, J. Zhan, G. Zou, A. Eychmüller and B. Cai, *Angew. Chem., Int. Ed.*, 2022, **62**, e202214487.
33 M. Dud, Z. Glasovac, D. Margetic and I. Piantanida, *New J. Chem.*, 2020, **44**, 11537–11545.
34 J. Liu, Y. Q. Sun, Y. Huo, H. Zhang, L. Wang, P. Zhang, D. Song, Y. Shi and W. Guo, *J. Am. Chem. Soc.*, 2014, **136**, 574–577.
35 Y. Zheng, H. Yang, L. Zhao, Y. Bai, X. Chen, K. Wu, S. Liu, Y. Shen and Y. Zhang, *Anal. Chem.*, 2022, **94**, 3296–3302.
36 K. Chen, J. Zhao, X. Li and G. G. Gurzadyan, *J. Phys. Chem. A*, 2019, **123**, 2503–2516.

37 C. Cheng, Y. Huang, X. Tian, B. Zheng, Y. Li, H. Yuan, D. Xiao, S. Xie and M. M. F. Choi, *Anal. Chem.*, 2012, **84**, 4754–4759.
38 R. Liu, C. H. Mak, X. Han, Y. Tang, G. Jia, K.-C. Cheng, H. Qi, X. Zou, G. Zou and H.-Y. Hsu, *J. Mater. Chem. A*, 2020, **8**, 23803–23811.
39 D. Zhong, S. Liu, L. Yue, Z. Feng, H. Wang, P. Yang, B. Su, X. Yang, Y. Sun and G. Zhou, *Chem. Sci.*, 2024, **15**, 9112–9119.
40 Z. Zhu, C. Zeng, Y. Zhao, J. Ma, X. Yao, S. Huo, Y. Feng, M. Wang and X. Lu, *Angew. Chem., Int. Ed.*, 2023, **62**, e202312692.
41 S. Liu, Q. Zhang, L. Zhang, L. Gu, G. Zou, J. Bao and Z. Dai, *J. Am. Chem. Soc.*, 2016, **138**, 1154–1157.
42 Z. Ding, B. M. Quinn, S. K. Haram, L. E. Pell, B. A. Korgel and A. J. Bard, *Science*, 2002, **296**, 1293–1297.
43 Y. He, L. Yang, F. Zhang, B. Zhang and G. Zou, *J. Phys. Chem. Lett.*, 2018, **9**, 6089–6095.
44 X. Ning, B. Lu, Z. Zhang, P. Du, H. Ren, D. Shan, J. Chen, Y. Gao and X. Lu, *Angew. Chem., Int. Ed.*, 2019, **58**, 16800–16805.
45 X. Ning, P. Du, Z. Han, J. Chen and X. Lu, *Angew. Chem., Int. Ed.*, 2020, **60**, 3504–3509.
46 C. Zachäus, F. F. Abdi, L. M. Peter and R. van de Krol, *Chem. Sci.*, 2017, **8**, 3712–3719.
47 X. Ning, D. Yin, Y. Fan, Q. Zhang, P. Du, D. Zhang, J. Chen and X. Lu, *Adv. Energy Mater.*, 2021, **11**, 2100405.
48 Q. Han, C. Wang, P. Liu, G. Zhang, L. Song and Y. Fu, *Chem. Eng. J.*, 2021, **421**, 129761.
49 J. Guo, W. Feng, P. Du, R. Zhang, J. Liu, Y. Liu, Z. Wang and X. Lu, *Anal. Chem.*, 2020, **92**, 14838–14845.
50 J. You, S. Lee, H. J. Tark, M. J. Nang, J. H. Oh and I. Choi, *Anal. Chem.*, 2022, **94**, 5521–5529.
51 Y. Gao, T. A. Konovalova, J. N. Lawrence, M. A. Smitha, J. Nunley, R. Schad and L. D. Kispert, *J. Phys. Chem. B*, 2003, **107**, 2459–2465.